

# PREDICTING THE COMPRESSION STRENGTH OF IMPACT-DAMAGED SANDWICH PANELS

James Ratcliffe<sup>1</sup>, Wade Jackson<sup>2</sup>, Jeffery Schaff<sup>3</sup>

<sup>1</sup> *National Institute of Aerospace, 144 Research Drive, Hampton, VA 23666, USA*

<sup>2</sup> *Army research laboratory, Vehicle Technology Directorate, NASA Langley Research Center, 2 West Reid Street, Hampton, VA 23681, USA*

<sup>3</sup> *Sikorsky Aircraft, Mail Stop: S352A, 6900 Main Street, Stratford CT 06615, USA*

**SUMMARY:** The objective of this work was to develop a technique for predicting the residual compression strength of sandwich panels containing impact damage in one facesheet. The technique was tailored to predict the strength of specimens that exhibit a failure mode involving the formation of kink bands at locations of peak strain in the region of impact damage. Under continued compression loading, the kink bands propagate in a stable manner perpendicular to the applied load. When a critical kink-band length is reached, growth becomes unstable corresponding to panel failure. The analysis follows in two sections. The first section calculates the far-field stress required for stable kink-band growth and the second calculates that required for unstable growth. The residual strength prediction is made when the stress for stable growth becomes equal to that for unstable kink-band growth. Initial comparisons between analysis and experiment show good agreement.

**KEYWORDS:** Residual compression strength prediction, Compression after impact, Sandwich.

## INTRODUCTION

Sandwich construction is an efficient means of providing structural components with high bending stiffness relative to their overall weight. The interaction, however, between the stiff facesheet and low-density core results in numerous possible failure modes such as core crushing, facesheet wrinkling, and facesheet/core debonding [1]. Characterizing the performance of sandwich structures is further complicated when damage, such as caused by an impact, is introduced into the facesheet material. For many applications such as rotorcraft, the airframe skins are designed to damage tolerance requirements. A concern for rotorcraft structure is the residual compression strength of sandwich structure containing low-velocity impact damage on the external facesheet. In Ref. 2, a series of compression tests was undertaken on sandwich panels containing varying degrees of impact damage on one facesheet. Specimens containing open holes in one facesheet were also tested for comparison to the impact-damaged specimens. During tests on some specimens, a kink-band (local out-of-plane buckling of the load-direction fibers in the laminate) was observed to propagate from the regions of peak strain around the impacted region. Stable propagation of the kink band took place perpendicular to the axial compressive load as the load was increased. After a critical kink-band length was reached, kink-band growth became unstable resulting in panel failure. This failure mode, termed kink-band propagation failure, is shown in Fig. 1. The kink-band growth failure mode was also observed in all specimens with an open hole. This failure mode has been reported in other work [3].

Kink-band propagation failure in sandwich construction has received some attention in the research community. In Ref. 4, the stress concentrations developed near the impact-damaged region in a sandwich panel facesheet were calculated. The damaged region was modeled as an inclusion of reduced stiffness. Failure was predicted based only on the estimated stress concentration factor. During studies into the compression failure of sandwich panels containing through-thickness slits, (Refs. 5 and 6), kink bands of microbuckled 0-degree fibers (fibers aligned to the load direction) were observed propagating from the slit edges. Following the methodology of previous work [7], the kink bands were modeled as cracks bridged by the damaged material close to the crack tip. An extension of Dugdale's analysis (Ref. 8) was then used to calculate the ultimate failure stress of the panel. A similar procedure was applied to sandwich panels containing through-thickness holes (Ref. 9) and was found to yield good agreement with experimental data.

The objective of this work was to develop a technique for predicting the residual compression strength of sandwich panels containing impact damage in one facesheet. The method assumed that specimens fail by the kink-band propagation mechanism. Only the impact-damaged facesheet was used to represent the sandwich panel, with the impacted area modeled as an open hole. A theoretical analysis developed in Ref. 7 for laminates was used for the residual compression strength prediction. The analysis proceeds in two stages, representing stable and unstable kink-band propagation. First, the average stress criterion [10] is used to calculate the far-field stress for stable kink-band growth. Second, linear elastic fracture mechanics (LEFM) is used to estimate the far-field stress required for unstable kink-band growth. A new type of fracture test was conducted to replicate kink-band propagation, from which a critical stress intensity factor was calculated and used in the LEFM calculations. The prediction method was calibrated against experimental residual compression strength values (Ref. 2) of sandwich panels containing an open hole in one facesheet or impact damage of an equivalent diameter to the open hole.

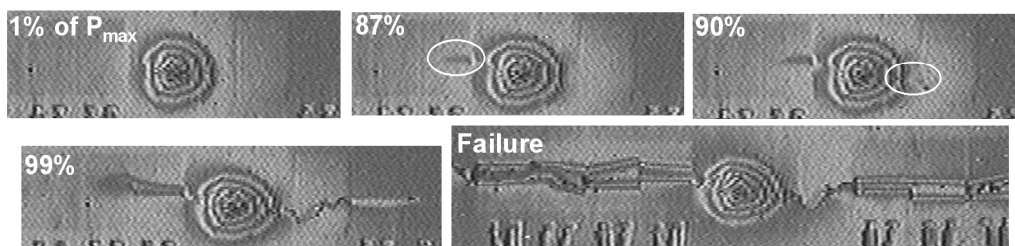


*Fig. 1: Shadow moiré images of kink band propagation failure mechanism [2]*

## RESIDUAL COMPRESSION STRESS PREDICTION METHOD

### Specimen and Materials

Compression strength predictions were compared to the strengths measured in a previous study [2]. The sandwich specimens were nominally 140 mm-square panels with a 25 mm-thick core, Fig. 2. The facesheets consisted of three plies of plain-weave carbon/epoxy fabric in the layup  $[(\pm 45)/(0/90)/(\pm 45)]$ . Each ply had a nominal cured thickness of 0.2 mm. Nomex honeycomb with density of  $48.1 \text{ kg/m}^3$  and a cell size of 3.175 mm was used for the core material. The ends of the core material were potted with a syntactic foam (Epocast 1614) to prevent specimen damage at the load introduction points. Holes were drilled into the center of one facesheet for open-hole compression testing. In other specimens, impact damage was introduced into one facesheet using a drop-weight impactor with a 12.7 mm-diameter hemispherical tip [2]. Specimens of interest in the current study contained 6.35 mm-diameter holes or impact damage with an equivalent diameter. Properties of the fabric, facesheet, core, and potting material are listed in Table 1.

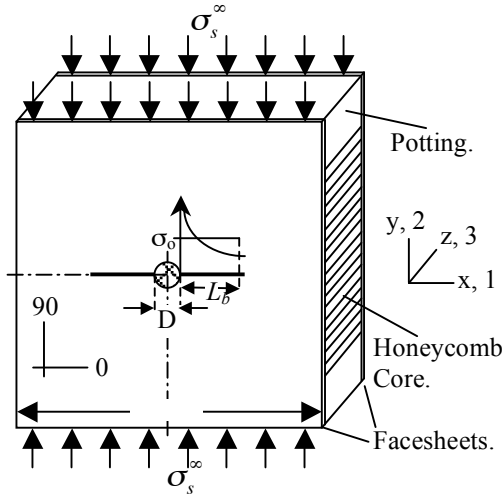


Fig. 2: Sandwich specimen configuration

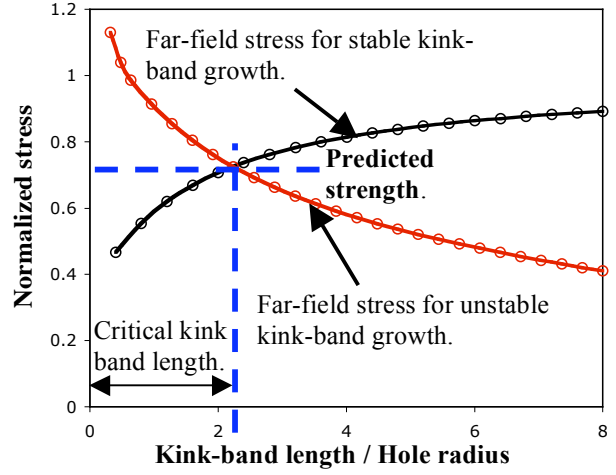


Fig. 3: Schematic of residual strength prediction

Table 1. Properties of sandwich specimen materials

	$E_{11}$ [GPa]	$E_{22}$ [GPa]	$G_{12}$ [GPa]	$\nu_{12}$	$t$ [mm]
Single ply carbon/epoxy plain weave fabric [11]	71.73	71.73	4.48	0.040	0.20
Face-sheet <sup>a</sup> [(±45)/(0/90)/(±45)]	41.75	41.75	24.48	0.441	0.57
Nomex honeycomb [12]	$E = 126.9 \text{ MPa}, \nu = 0.30$				25.40

<sup>a</sup>Theoretical properties determined using laminated plate theory.

### Far-Field Stress for Stable Kink-Band Growth

In this first step of the analysis, the far-field stress required for stable kink-band propagation,  $\sigma_s^\infty$ , was calculated. For simplicity in the analysis, only the impact-damaged facesheet was considered. An adjustment to the normal stresses adjacent to the open hole was made to accommodate for the difference in load transfer between the intact and damaged facesheets of the sandwich specimen. This adjustment is described in detail in Ref. [13]. It was assumed that load is not transferred through the core, as the core stiffness in the load direction is small in comparison to that of the facesheets. The stress field surrounding the impact region was approximated to that developed around an open hole. Initiation of the kink bands was therefore assumed to occur at the edges of the impact region, corresponding to the location of the peak strain. Upon further loading, the kink bands were assumed to grow in a stable fashion until a critical length ( $l_c$ ) is reached, after which the propagation becomes unstable. Kink-band growth was assumed to be symmetric about the center of the sandwich specimen. The far-field stress for stable kink-band growth,  $\sigma_s^\infty$ , was calculated using an average stress criterion [10], which states that kink-band growth will occur when the average stress across a given length becomes equal to the unnotched compression strength ( $\sigma_0$ ) of the sandwich panel. This is illustrated in Fig. 2, which highlights the decay in stress at distances further from the hole edges. An approximate, two-dimensional analytical method was selected for calculating the stress field in the vicinity of the open hole. The approach is based upon an analytical solution for stress distribution in an infinite, anisotropic plate containing an open hole that is loaded in tension [14]. According to Ref. 14, the normal stress in the direction of the applied load and in the vicinity of the open hole,  $\sigma_y$ , is defined by:

$$\sigma_y(\xi) \approx \sigma_s^\infty \left[ 1 + \frac{1}{2} \xi^{-2} + \frac{3}{2} \xi^{-4} - \frac{(K_T - 3)}{2} (5\xi^{-6} - 7\xi^{-8}) \right] \quad (1)$$

where  $\sigma_s^\infty$  is the far-field stress and  $\xi = (R+l_b)/R$ . The quantities  $l_b$  and  $R$  are the kink-band length and hole radius, respectively.  $K_T$  is the stress concentration factor at the boundary of the open hole (at  $\xi = 1$ ), and is defined in Ref. 15.

The approximation for  $\sigma_y$  in Eqn. 1 was then applied to the average stress criterion. At this stage of the analysis,  $\sigma_y$  was calculated at various increments of distance from the hole boundary along the expected path of kink-band growth (termed as the virtual kink band). An applied far-field stress of unity was assumed in Eqn. 1, and thus the far-field stress required to cause stable kink-band propagation, as dictated by the average stress criterion was calculated as:

$$\sigma_s^\infty(\xi) = \left( \frac{\sigma_i^\infty}{\sigma_{ave}(\xi)} \right) \sigma_o \quad (2)$$

where  $\sigma_o$  is the strength of the unnotched sandwich panel,  $\sigma_i^\infty$  is the unit far-field stress,  $\sigma_{ave}$  is the average stress over a given distance from the hole, and  $\sigma_s^\infty$  is the far-field stress required for stable growth of the kink band. The stress,  $\sigma_{ave}$ , was calculated by integrating the normal stresses over the virtual kink-band length then dividing the integral by the virtual kink-band length. This calculation procedure was repeated for a range of virtual kink-band lengths. Subsequently, the far-field stress values needed for stable kink-band propagation were plotted versus kink-band length as illustrated in Fig. 3.

### Far-Field Stress for Unstable Kink-Band Growth

The second step of the residual compression strength prediction method used LEFM. The kink band was modeled as a crack emanating from the edges of the open hole in the facesheet. The onset of unstable kink-band growth was assumed to take place when the strain energy stored in the vicinity of the kink-band tip was equal to the fracture toughness of the facesheet through which the kink band propagates. Using LEFM, the critical far-field stress,  $\sigma_u^\infty$ , needed for unstable growth of the kink-band is given by [16]:

$$\sigma_u^\infty = \frac{K_{Ic}}{\sqrt{\pi l_b} f(l_b/R)} \quad (3)$$

where  $f(l_b/R)$  is the boundary correction factor, and  $K_{Ic}$  is the fracture toughness of the facesheet.

The boundary correction factor was calculated from 2D finite element analyses of the facesheet containing an open hole with cracks emanating from the hole edges. Using x-axis symmetry, half the facesheet was modeled. A typical mesh consisted of approximately 1600 four-node shell elements and 1700 nodes. Load was applied using prescribed displacements at the nodes on the upper and lower ends of the model. Nodes along the x-axis symmetry line were constrained from translation in the x-direction and rotations about the y and z-directions (see coordinate system in Fig. 2). Tension loading was applied on the assumption that the change in strain energy release rate with crack length is the same in tension and compression. A similar assumption was made in the analysis of Ref. 7. For a given hole diameter, the

analysis was repeated over a range of crack (kink band) lengths up to the maximum length of interest. Virtual crack closure technique (VCCT) [17] was then used to calculate the strain energy release rate,  $G$ , for each kink–band length. The stress intensity factor,  $K$ , was then calculated from each analysis using the following relation between  $K$  and  $G$  for an orthotropic plate [16]:

$$G = \left[ \frac{1}{2E_1E_2} \right]^{\frac{1}{2}} \left[ \left( \frac{E_1}{E_2} \right)^{\frac{1}{2}} + \frac{E_1}{2G_{12}} - \nu_{12} \frac{E_1}{E_2} \right]^{\frac{1}{2}} K^2 \quad (4)$$

where  $E_1$ ,  $E_2$  are the in-plane moduli,  $G_{12}$  is the in-plane shear modulus, and  $\nu_{12}$  is the Poisson's ratio of the facesheet. The subscripts correspond to the coordinate system shown in Fig. 2. The boundary correction factor,  $f(l_b/R)$ , was then calculated for each kink–band length using the relation below:

$$f(l_b/R) = \frac{K}{\sigma^\infty \sqrt{\pi l_b}} \quad (5)$$

where  $\sigma^\infty$  is the far-field stress applied in the finite element models. A comparison was made of the  $f(l_b/R)$  values calculated from the finite element analyses with values calculated from the known solution for an isotropic plate [18]. The facesheet detailed in Table 1 with a 6.35 mm open hole was modeled in the analyses. Fracture toughness of the facesheet was determined via a new test called the compact compression test [19]. A description of this test method is given in the proceeding section. The remote stress for unstable kink-band growth was then calculated using Eqn. 3 for a range of kink-band lengths and plotted as a function of kink-band length, as illustrated in Fig. 3.

### Fracture Toughness of Sandwich Panel Facesheets

The fracture toughness,  $K_{Ic}$ , of the facesheet material was measured using a new test called the compact compression test [19]. The compact compression specimen was designed specifically for inducing stable kink-band propagation in the sandwich panel facesheets. A schematic of the specimen is given in Fig. 4. Specimens are loaded in compression until a kink band is formed and grows approximately 10 mm, after which the specimen is unloaded.

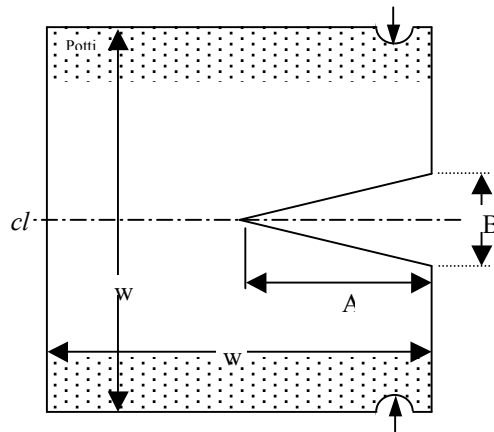


Fig. 4: Configuration of compact compression specimen

The specimen load-displacement response is recorded during the complete load cycle. The specimen is reloaded and the kink-band propagated a further 10 mm and then unloaded. This procedure is repeated up to seven times. The critical strain energy release rate,  $G_c$ , corresponding to each increment of kink-band growth was calculated using an areas method:

$$G_c = \frac{1}{b} \frac{dU}{da} \quad (6)$$

where  $dU$  is the strain energy dissipated during kink–band propagation,  $da$  is the increment in kink-band extension, and  $b$  is the width of the facesheet (doubled as kink-band growth takes place through both facesheets of the sandwich specimen). The relation in Eqn. 4 (assuming  $G = G_c$ ) was then used to calculate the corresponding fracture toughness,  $K_{Ic}$ . This calculation was repeated for each increment of kink-band extension that took place during a test. A complete description of the specimen preparation and test method is given in Ref. 19.

### Calibration of Residual Compression Strength Prediction Method

The current method was used to predict residual compression strength of sandwich panels tested in Ref. 2. Details of the sandwich configuration were given in the ‘‘Specimen and Materials’’ section. In Ref. 2, compression tests were conducted on panels containing 6.35 mm holes, located centrally in one of the facesheets. In other specimens, impact damage was introduced into one facesheet using a drop-weight impact device. The effective diameter of the subsequent impact damage was determined by measuring the distance between kink bands produced during the compression tests (see Fig. 1), and was found to be approximately 6.35 mm. Both the impact-damaged and open-hole specimens exhibited kink-band propagation failure during compression tests. Compression tests were also conducted on intact specimens yielding an unnotched compression strength value. Table 2 contains a summary of the compression strength data measured in Ref. 2. In the table, the strength of the specimens containing impact damage is referred to as CAI (compression after impact) and represents an average of six specimens. The other two strength values represent an average of two tests. The steps outlined in the preceding section were then used to calculate the residual compression strength of the sandwich panel. A comparison was made between predicted residual strength from the current study and experimental values of Ref. 2.

*Table 2: Compression strength data [2] (cov in parenthesis)*

Unnotched strength[MPa] (cov)	Open-hole strength[MPa]	CAI strength [MPa]
288 (0.14)	229 (0.06)	218 (0.28)

## RESULTS AND DISCUSSION

### Calculation of Boundary Correction Factor $f(l_b/R)$

The  $f(l_b/R)$  factors calculated from the finite element analyses of the facesheet with a 6.35 mm open hole are presented in Table. 3. The  $f(l_b/R)$  factors from the finite element analyses are also compared in the table to values obtained from a known solution for  $f(l_b/R)$  [18]. There is little difference between the two sets of values and therefore the known solution is used in this analysis. Similar findings were reported in Ref. 7.

*Table 3: Comparison of  $f(l_b/R)$  values of open-hole plate with cracks growing from hole edges*

$l/R$	0.1	0.2	0.3	0.4	0.5	0.6	0.8	1.0
$f(l_b/R)$ Ref. 18	2.73	2.41	2.15	1.96	1.83	1.71	1.58	1.45
$F(l_b/R)$ FEA	2.69	2.41	2.19	2.03	1.89	1.79	1.64	1.52

## Fracture Toughness of Sandwich Panel Facesheets

A set of typical load-displacement records from compact compression tests is presented in Fig. 5a. Load and displacement values are normalized by the maximum load and displacement from Run 1 respectively. The specimen response was reasonably linear until the kink bands grew longer than 25 mm from the notch. After this kink-band length, load-displacement response was nonlinear which was attributed to the damage induced along the kink band during the loading cycle. Critical strain energy release rates,  $G_c$ , were calculated for each kink-band growth increment using Eqn. 6. The critical strain energy release rates are plotted as a function of kink-band length in Fig. 5b. Strain energy release rate and kink-band length are normalized by the corresponding maximum values. The values were taken from all five tests conducted. The critical energy release rate remained reasonably constant over the first 25 mm of kink-band growth, although the scatter in the data was significant. After this length,  $G_c$  began rising sharply. At longer kink-band lengths, energy-dissipating mechanisms in addition to kink-band formation were likely to be taking place (suggested by nonlinearity of load-displacement response). Maximum kink-band lengths observed during compression tests (Ref. 2) on the sandwich specimens modeled in the current investigation were less than 25 mm. This corresponds to the kink-band length range over which a relatively constant critical

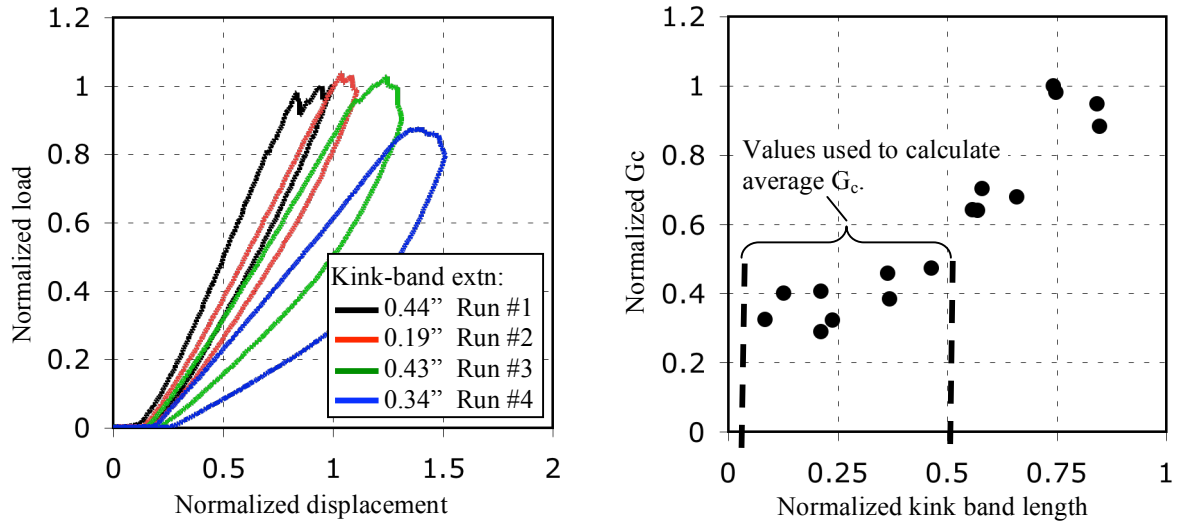


Fig. 5: (a) Load-displacement response of a compact compression specimen (b) Critical strain energy release rate versus kink band length

strain energy release rate was measured. Consequently, the arithmetic mean of the values highlighted in Fig. 5b were used to calculate a mean critical strain energy release rate,  $\bar{G}_c$ . This value was then used in the current analysis. The mean critical strain energy release rate was 36100 N/m with a standard deviation of 5600 N/m. The corresponding mean fracture toughness of the facesheet,  $\bar{K}_c$ , (assuming  $G = \bar{G}_c$  in Eqn. 4 and facesheet properties in Table 1) was 42.4 MPa-m<sup>1/2</sup>. This value is comparable to toughness values reported in the literature for carbon/epoxy laminates with a stacking sequence of ( $\pm 45/0$ )<sub>n</sub> (Ref. 7). For analysis purposes, critical strain energy release rates were calculated based on one standard deviation below ( $\bar{G}_c^{\text{lower}} = 30500$  N/m) and above ( $\bar{G}_c^{\text{upper}} = 41700$  N/m)  $\bar{G}_c$ . A summary of the fracture data generated from the compact compression tests is presented in Table 3.

Table 3: Fracture toughness data

$\bar{G}_c$ [N/m]	$\bar{K}_c^{\text{lower}}$ [MPa-m <sup>1/2</sup> ]	$\bar{K}_c$ [MPa-m <sup>1/2</sup> ]	$\bar{K}_c^{\text{upper}}$ [MPa-m <sup>1/2</sup> ]
36089 ( $\pm 5600$ )	38.9	42.4	45.5

## Calibration of Residual Compression Strength Prediction Method

The residual strength of the sandwich specimen containing a 6.35 mm open hole in one facesheet was calculated using the current analysis. The far-field stresses needed for stable and unstable kink-band growth were plotted as functions of kink-band length. The plots were superimposed and are presented in Fig. 6. Both far-field stress values have been normalized by the unnotched strength of the sandwich panel (288 MPa) and the kink-band length is normalized by the hole radius (6.35 mm). The mean fracture toughness,  $\bar{K}_{Ic}$ , obtained from the compact compression tests was used in calculating the result given in Fig. 6. The intersection of the curves corresponded to a far-field stress-to-unnotched compression strength ratio of 0.738. The corresponding predicted residual strength and critical kink-band length values were 212 MPa and 7.1 mm, respectively. The residual strength prediction is in good agreement with the corresponding experimental values of 218 MPa for impact-damaged specimens and 229 MPa for open-hole compression specimens. The error between the predicted residual strength (using  $\bar{K}_{Ic}$ ) and the experimental value, was approximately  $-3\%$  for impact-damaged specimens and  $-4.0\%$  for the open-hole specimens. The critical kink-band length was not documented in Ref. 2 for the sandwich configuration modeled, so a determination of the accuracy of the predicted value was not made.

The residual compression strength was also calculated using the upper and lower values of facesheet fracture toughness,  $\bar{K}_{Ic}^{upper}$  and  $\bar{K}_{Ic}^{lower}$  respectively (Table 3). The resulting strength predictions are given in Table 4. A 15% reduction in fracture toughness (difference between  $\bar{K}_{Ic}^{lower}$  and  $\bar{K}_{Ic}$ ) resulted in a 4% decrease in the predicted strength value. Similarly, a 15% increase in fracture toughness yielded a 3% increase of the strength prediction. The results indicated that the residual strength prediction was moderately insensitive to the experimental scatter of the facesheet fracture toughness values. Furthermore, all the predicted strength values were conservative estimates of the corresponding experimental value.

Table 4: Predicted and experimental values

	Predicted values			Open-hole (Ref. 2)	CAI (Ref. 2)
	Lower	Mean	Upper		
$\sigma_c^\infty$ [MPa]	204	212	219	229	218
$l_c$ [in]	0.24	0.28	0.32		

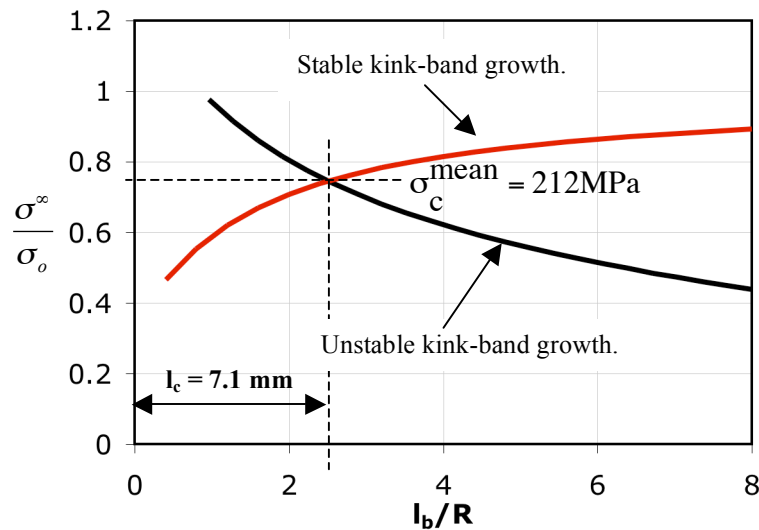


Fig. 6: Prediction of residual compression strength of sandwich specimen with  $D/w = 0.045$ .

## CONCLUDING REMARKS

A technique has been developed for predicting the residual compression strength of impact-damaged sandwich panels that exhibit the kink-band propagation failure mode. The technique models the impact-damaged sandwich panel as a plate with an open hole. Far-field stress needed for stable kink-band growth was calculated using plate theory. The far-field stress required for unstable kink-band growth was calculated using LEFM.

A fracture specimen was designed to replicate kink-band growth and determine the corresponding facesheet fracture toughness. Initial findings show that the fracture test yields moderately constant values of fracture toughness over a limited kink-band length range (up to 25 mm) for the sandwich configuration currently investigated. The boundary correction factor,  $f(l_b/R)$ , for the fracture toughness calculation, was determined for the facesheet of the sandwich panel investigated. The values were similar to those calculated for an isotropic plate [18]. The current analysis method was calibrated against experimental values of residual compression strength of a sandwich panel comprised of a Nomex honeycomb core reinforced with carbon/epoxy plain-weave fabric facesheets. The residual compression strength of specimens with a 6.35 mm-diameter open hole were predicted. Measured residual compression strength of sandwich panels containing impact damage with an equivalent hole diameter of 6.35 mm was also compared with the predicted value. The predicted residual strength of the sandwich specimen studied was in good agreement with the residual strengths of the impact-damaged specimens and those containing 6.35 mm open holes. The sensitivity of the predicted residual strength to the scatter in measured facesheet fracture toughness values was found to be small. Each predicted strength value (calculated over two standard deviations of fracture toughness values) were conservative estimates of the measured strengths.

## ACKNOWLEDGEMENTS

This research was partially funded by the Aviation Applied Technology Directorate under Technology Investment Agreement No. DAAH10-02-2-0001. The U.S. Government is authorized to reproduce and distribute reprints for Government purposes notwithstanding any copyright notation thereon. This work was conducted in association with the Rotorcraft Industry Technology Association (RITA).

## REFERENCES

1. Allen, G.H., "Analysis and Design of Structural Sandwich Panels", Pergamon Press, 1969.
2. Cvitkovich, M.K., and Jackson, W.C., "Compressive Failure Mechanisms in Composite Sandwich Structures", *Journal of the American Helicopter Society*, Vol.44(4), 1999, pp.260-268
3. Tomblin, J.S., Raju, K.S., and Smith, B.L., "Damage Resistance and Tolerance of Sandwich Airframe Structures", *FAA Materials and Structures R&D Workshop*, 2003.
4. Kassapoglou, C., "Compression Strength of Composite Sandwich Structures After Barely Visible Impact Damage", *ASTM Journal of Composites Technology and Research*, Vol.18(4), 1996, pp.274-284.
5. Toribio, M.G., Marizo, J.M., and Spearing, S.M., "Compressive Failure of Notched Composite-Honeycomb Sandwich Panels", *Proc. 12<sup>th</sup> International Conference on Composite Materials*, Paris, 1999.

6. Marizo, J.M., and Spearing, M.S., "Damage Modeling of Notched Graphite/Epoxy Sandwich Panels in Compression", *Applied Composite Materials*, Vol.8(3), 2001, pp.191-216.
7. Soutis, C., and Fleck, N.A., "Static Compression Failure of Carbon Fibre T800/924C Composite Plate with a Single Hole", *Journal of Composite Materials*, Vol.24, 1990, pp.536-558.
8. Dugdale, D.S., "Yielding of Steel Sheets Containing Slits", *Journal of the Mechanics and Physics of Solids*, 1960, pp.118-136.
9. Toribio, M.G., and Spearing, S.M., "Compressive Response of Notched Glass-Fiber Epoxy/Honeycomb sandwich Panels", *Composites: Part A*, Vol.32, 2001, pp.859-870.
10. Whitney, J.M. and Nuismer, R.J., "Stress Fracture criteria for Laminated Composites Containing Stress Concentrations", *Journal of Composite Materials*, Vol.8, 1974, pp.253-265.
11. Krueger, R., Paris, I.L., O'Brien, T.K., and Minguet, P.J., "Fatigue Life Methodology for Bonded Composite Skin/Stringer Configurations", *Journal of Composites Technology and Research*. Vol.24(2) , 2002, p. 56-79.
12. Hexcel Composites, HexWeb HRH-10 Product Data Sheet, Hexcel Corp, 2003.
13. Ratcliffe, J.G., Jackson, W.C. and Schaff, J.R., "Compression Strength Prediction of Impact-Damaged Sandwich Panels", *To be submitted as a NASA TM*.
14. Konish, H.J., and Whitney, J.M., "Approximate Stresses in an Orthotropic Plate Containing a Circular Hole", *Journal of Composite Materials*, Vol.9, 1975, pp.157-166.
15. Lekhnitskii, S.G., "Theory of Elasticity of an Anisotropic Elastic Body", Holden-Day, Inc, San Francisco, 1963, pp.163-170.
16. Paris, P.C., and Sih, G.C., "Stress Analysis of Cracks", *Fracture Toughness Testing and Its Applications*, ASTM STP 381, 1965, pp.30-83.
17. Rybicki, E.F., and Kanninen, M.F., "A Finite Element Calculation of Stress Intensity Factors by a Modified Crack Closure Integral", *Engineering Fracture Mechanics*, Vol.9, 1977, pp.931-938.
18. Bowie, O.L., "Analysis of An Infinite Plate Containing Radial Cracks Originating from the Boundary of an Internal Circular Hole", *Journal of Mathematics and Physics*, Vol.35, 1956, pp.60-71.
19. Jackson, W.C. and Ratcliffe, J. G., "Measurement of Fracture Energy for Kink-Band Growth in Sandwich Specimens", *Proc 2<sup>nd</sup> International Conference on Composites testing and Model Identification*, 21<sup>st</sup>-23<sup>rd</sup> September 2004, Paper 24.